Cooperative Cathodes for Enhanced Hexavalent Chromium Reduction and Electricity Generation in Bioelectrochemical Reactor with Simultaneous Sludge Degradation

Hang Yu
Dalian Maritime University https://orcid.org/0000-0002-7432-4556
Qingliang Zhao (zhql1962@163.com)
Harbin Institute of Technology
Yuhui Cao
Dalian Maritime University
Tiantian Sun
Dalian Maritime University
Zhuyuan Liang
Harbin Institute of Technology
Weifeng Liu
Dalian Maritime University
Yimin Zhu
Dalian Maritime University

Research Article

Keywords: Bioelectrochemical reactor, hexavalent chromium, cooperative cathodes, excess sludge, electron flux, electrochemically active microorganisms

Posted Date: October 22nd, 2021

DOI: https://doi.org/10.21203/rs.3.rs-961487/v1

Cooperative Cathodes for Enhanced Hexavalent Chromium Reduction and Electricity Generation in Bioelectrochemical Reactor with Simultaneous Sludge Degradation

Hang Yu[a], Qingliang Zhao[b,*], Yuhui Cao[a], Tiantian Sun[a], Zhuyuan Liang[b,c], Weifeng Liu[a], Yimin Zhu[a,*]

a Collaborative Innovation Center for Vessel Pollution Monitoring and Control, Dalian Maritime University, Dalian 116026, China

b State Key Laboratory of Urban Water Resources and Environments (SKLURE), School of Environment, Harbin Institute of Technology, Harbin 150090, China

c Investment Development Department, CIFI GROUP, Hefei 230081, China

* Corresponding author. Tel: +86 451 8628 3017; Fax: +86 451 8628 3017. E-mail address: qlzhao@hit.edu.cn (Qingliang Zhao); Tel: +86 411 84726992; Fax: 86 411 84726992. E-mail address: ntp@dlmu.edu.cn (Yimin Zhu).

Abstract： In a typical microbial electrochemical system (MES) with dual-chamber for Cr(VI) reduction, it was faced with the decline of Cr(VI) reduction efficiency after several cycles of operation, which limited the continuous and effective Cr(VI) reduction of MES. In this study, a novel bioelectrochemical reactor assembled with cooperative cathodes of chemical cathode and bio-cathode (BER_{CC}) and with excess sludge as anodic substrate was designed to solve the problem. Comparative study of BER_{CC} and BER with dual chemical cathodes (BER_{DC}) revealed that BER_{CC} broke through the limitation of Cr(VI) reduction decline for cycles of operation and improved performance of electricity generation. Both the Cr(VI) reduction rate and the power density were increased with the decrease of pH and the increase of TCOD and initial Cr(VI) concentration. Cooperative cathodes stimulated the growth of electrochemically active microorganisms in the anodic biofilm and produced 8.21±0.64 mg Coulomb/(L·h) more electrons than dual chemical cathodes, which enhanced the electrons for electricity generation and Cr(VI) reduction by about 58.3% and 56.1±5.6% in BER_{CC} than those in BER_{DC}.

Keywords： Bioelectrochemical reactor, hexavalent chromium, cooperative cathodes, excess sludge, electron flux, electrochemically active microorganisms

1. Introduction

Microbial electrochemical system (MES) is an emerging platform technology, which combines electrochemical systems with microbial processes. This technology has been extensively studied and intensively developed for remediation of wastewater (Jadhav et al. 2017), soil (Chen *et al*. 2015), sediment (Wan *et al*. 2018), CO_2 (Rodrigues et al. 2019), etc. Remediation of hexavalent chromium [Cr(VI)] contaminated wastewater has been one of the widely researched fields for MES (Wang et al. 2008; Kim et al. 2017; Wang et al. 2017; Han et al. 2018; Li and Zhou 2019)，where the electrochemically active microorganisms (EAMs) use electrodes as electron acceptors/donors via extracellular electron transfer and close circuit (Logan et al. 2006; Shi et al. 2016; Rabaey et al. 2009). Microbial electrochemical Cr(VI) reduction mainly bases on cathodic reduction with abiotic/biotic cathode, reflecting the advantages of sustainability and low-cost (Sophia and Saikant 2016).

In a typical MES with dual-chamber for Cr(VI) reduction, the anodic reaction equation (taking glucose as the example of anodic substrate) and the cathodic reaction equation were shown in Eq.(1) and Eq.(2), respectively (Wang et al. 2008).

$$C_6H_{12}O_6 + 6H_2O \rightarrow 6CO_2 + 24H^+ + 24e^- \quad (1)$$

$$Cr_2O_7^{2-} + 14H^+ + 6e^- \rightarrow 2Cr^{3+} + 7H_2O \quad (2)$$

At the early stages of the reaction process, the initial high concentrations of Cr(VI) and H^+ can positively affect the cathodic reaction and lead to a high Cr(VI) reduction rate. High concentration of anodic substrate at early stages also promotes the activity of EAMs and accelerates the substrate degradation. Thus, lots of electrons can be produced during organic matter degradation in the anodic chamber to support fast

cathodic Cr(VI) reduction, as shown in Eq.(1) and Eq.(2). As the reaction of MES progresses, however, the consumption of Cr(VI) and H^+ in the cathodic chamber results in the decline of motivation force from the cathodic reaction. After several Cr(VI) reduction cycles, the cathodic reduction efficiency gradually decreases, and the cathodic potential declines slowly with it, which also reduces the activity of EAMs in the anodic chamber and has a negative influence on the electricity generation finally (Xafenias et al. 2014). Similar changes were also shown in other studies. In a dual-chamber microbial fuel cell (MFC) with conductive polymer-mediated Cr(VI) reduction, Cr(VI) was completely removed for the initial two cycles, but less than 80% of removal efficiency was generated for the 3rd cycle, and the removal efficiency dropped to 60% for the 4th cycle (Pang et al. 2013) . In another dual-chamber MFC with graphene/biofilm composites for Cr(VI) reduction, the removal efficiency was 58±0.5% for the 1st cycle, while the value was decreased to 45.2±4% for the 2nd cycle, and the value dropped to 15.5±1.3% for the 3rd cycle (Song et al. 2016). In a four-chamber microbial desalination cell for Cr(VI) reduction and salinity removal, the decrease of Cr(VI) concentration led to the drop in current density, which was gradually decreased along each Cr(VI) reduction cycle (An et al. 2014). These studies showed that MES was faced with the decline of Cr(VI) reduction efficiency after cycles of operation, which limited the continuous and effective Cr(VI) reduction of MES.

Using high organic concentration of anodic substrate is one of the solutions that supply abundant electrons for continuous and effective Cr(VI) reduction in MES. The anodic substrate is the electron donor of MES for current generation and cathodic reaction. Sludge, as a typical substrate with high concentration of organic matters, has

been reported to supply electrons for electricity generation steadily in MES. Jiang et al. (2009) positioned a two-chamber MFC with potassium ferricyanide as catholyte, which degraded excess sludge with stable and high electricity generation during operation of 40 h. Meng et al. (2019) invented a solid phase bioelectrochemical system, providing a method for simultaneous sludge compost, bioelectricity generation, and desalination with a relatively stable operational period of nearly 151 days (cell voltage > 0.6 V). Hence, MES with sludge as the anodic substrate can create the condition of sufficient electron donors for stable and high flow electron transfer. In our previous research, a bioelectrochemical reactor (BER) was constructed with sewage sludge as the anodic substrate and Cr(VI) as the catholyte, which paved the way for simultaneous treatment of sewage sludge and wastewater containing Cr(VI) (Yu et al. 2018).

Maintaining high activity of EAMs is the other solution that supplies electrons for continuous and effective Cr(VI) reduction in MES, which results in high performance of electricity generation. Due to the thermodynamic constraints, traditional MFC produced 1.14 V as determined by the NADH and pure oxygen redox potentials. Dual-cathode MFCs with two cathodes share the anode, incorporated an extra cathodic chamber flanked with the anodic chamber of dual-chamber MFCs and had higher electricity generation than that of dual-chamber MFCs (Jiang et al. 2011; Zhang and He 2012). A coupled MFC consisting of an oxic-biocathode MFC and an anoxic-biocathode MFC was implemented to remove carbon and nitrogen from synthetic wastewater simultaneously, which obtained a maximum COD removal rate of 98.8% and reached a power density of 14 W/m^3 net cathodic compartment and 7.2 W/m^3 net cathodic compartment, respectively (Xie et al. 2011). From here we infer

that electricity generation can be kept in the state of stable and continuous Cr(VI) reduction rate by cooperative cathodes, where bio-cathode was coupled to traditional dual-chamber MES. Bio-cathode not only lowered the cost of construction and operation of reactors, but also increased the operational sustainability (He and Angenent 2006; Rabaey and Keller 2008). Hence, coupling of bio-cathode and chemical cathode can be regarded as the appropriate cooperative cathodes. Nevertheless, few studies were relative to cooperative cathodes for enhancing the performance of Cr(VI) reduction in MES.

To obtain abundant electrons for continuous and effective Cr(VI) reduction in MES, we designed a novel BER assembled with cooperative cathodes of chemical cathode and bio-cathode as shown in Fig. 1a. Under this configuration with excess sludge as electron donors and both chemical cathode and bio-cathode as electron acceptors, which can keep the high performance of BER. The performances of BER with cooperative cathodes (BER_{CC}) and BER with dual chemical cathodes (BER_{DC}) were compared, to substantiate the feasibility of keeping high efficiency by cooperative cathodes of BER_{CC}. Afterwards, effects of the major impact factors [viz., Cr(VI) concentration and pH of catholyte and total chemical oxygen demand (TCOD) of excess sludge] on the performance of BER_{CC} were investigated. In addition, the distribution of electron flux and the structure of microbial community within BER_{DC} and BER_{CC} were analyzed. This study provides alternative technology for the continuous and efficient remediation of Cr(VI) contaminated wastewater and treatment of excess sludge.

2. Materials and methods

2.1 Configuration of BER_{CC} and BER_{DC}

The bioelectrochemical reactor with cooperative cathodes (BER_{CC}) consists of a cylindrical anodic chamber (Φ 80 mm×90 mm) and two cubic cathodic chambers (60 mm×70 mm×90 mm each) (Fig. 1a). The effective volumes of the anodic chamber and cathodic chamber in the BER_{CC} were 340 mL and 300 mL, respectively. Proton exchange membrane (PEM) (Nafion^{TM}117, DuPont Co., USA) separated the anodic chamber from the chemical cathodic chamber for preventing the Cr^{3+} produced in the chemical cathodic chamber from entering the anodic chamber, and the cation exchange membrane (CEM) (AMI-7001, Ultrex, USA) separated the anodic chamber from the bio-cathodic chamber in consideration of cost. All of the anode and cathodes were made of graphite fibre brushes (Φ 70 mm×70 mm for the anode and Φ 60 mm×70 mm for both cathodes) and titanium wires. The BER with dual chemical cathodes (BER_{DC}) possesses the same configuration with BER_{CC} as shown in Fig. 1b, which was applied as the control for experiments. Both chemical cathodic chambers were separated by PEMs from the anodic chamber. The BER_{CC} at open circuit was used as the control to reflect the role of adsorption for Cr(VI) removal.

Fig.1

2.2 Inoculation and operation

Excess sludge was used as the inoculum and the anodic substrate of the anodes of BER_{CC} and BER_{DC}, which was collected from the Harbin municipal wastewater treatment plant. The total chemical oxygen demand (TCOD), soluble chemical

157 oxygen demand (SCOD) and moisture content of the excess sludge were 22307±694
158 mg/L, 124.5±0.6 mg/L, 97.1±0.5%, respectively. For the start-up, both the inoculum
159 (excess sludge) for the anode and catholyte (potassium dichromate of 0.1 mol/L) for
160 the cathodes were both filled at the height of 70 mm and replaced every three days
161 until stable voltage was obtained in the reactor (Aelterman et al. 2006).
162
163 After start-up, the catholyte for the chemical cathodes of BER_{CC} and BER_{DC} was
164 changed to the aqueous solution prepared by dissolving $K_2Cr_2O_7$ in deionized water at
165 a pH of 2 (Wang et al. 2008). The catholyte for the bio-cathode of BER_{CC} included
166 nutritional salts, inoculated bacteria, and dissolved oxygen. The nutritional salts were
167 prepared as previously described (Rabaey et al. 2005). The inoculated bacteria were
168 collected from the catholyte of the bio-cathode of an MES in a good operating state.
169 Dissolved oxygen was continuously generated by the aerator at 200 mL/min (Fig. 1a).
170 All the experiments were in the mode of sequencing batch at 25±1℃. All of the
171 samples were analyzed in triplicate.
172
173 2.3 Analysis and calculation
174 The pH value and concentration of Cr(VI) of the catholyte and TCOD and SCOD
175 of excess sludge were measured based on the Standard Methods (APHA 2015; Yu, et
176 al. 2018). The precipitate produced during Cr(VI) reduction was observed by the
177 scanning electron microscope energy dispersive X-ray analysis (SEM-EDX) and
178 X-ray photoelectron spectroscopy (XPS). The voltage of BER_{CC} and BER_{DC} was
179 measured with an external resistance of 1000 Ω by a voltage collector. Polarization
180 curves were calculated according to the previous study (Logan and Regan 2006), and
181 the effective volume of the anodic chamber was used to calculate the power density

(Jiang et al. 2009). The production of methane and hydrogen was measured by titration and off-gas analysis (TOGA) sensor (Pratt et al. 2003; Virdis *et al*., 2009). The qualification of electron fluxes was realized as previously studied (Yu et al. 2018).

During the period of operation, a small amount of graphite fibres were collected from the anodes of BER_{CC} and BER_{DC} and the bio-cathode of BER_{CC} for DNA extraction. Total genomic DNA was extracted using a DNA Isolation Kit. The V3-V4 region of the bacterial 16S rRNA gene was amplified by the universal primers 341F (5′-CCCTACACGACGCTCTTCCGATCTG-3′) and 805R (5′-GACTGGAGTTCCTTGGCACCCGAGAATTCCA-3′) to analyze the structures of the bacterial communities. The sequences were computed with a similarity of 97%. Chao1 and Shannon index were used to estimate the levels of alpha diversity.

3. Results and discussion

3.1 Performances of BER_{CC} and BER_{DC}

To reveal the advantages of cooperative cathodes on hexavalent chromium reduction, electricity generation, and sludge degradation, the performances of BERs with cooperative cathodes (BER_{CC}) and chemical dual-cathodes (BER_{DC}) were compared.

3.1.1 Performance of hexavalent chromium reduction

As shown in Fig. 2a, Cr(VI) was almost reduced completely within 55.5 h and 57.5 h in BER_{CC} and BER_{DC} for the 1st Cr(VI) reduction cycle, respectively. After it, the Cr(VI) reduction rates of BER_{DC} were gradually decreased, and it took 102.5 h

and 66.0 h for BER_{DC} to reduce Cr(VI) by 72.5±2.8% and 52.1±1.8%, respectively. The Cr(VI) reduction efficiency dropped to 39.9±1.3% for the 5th cycle. In another dual-chamber MFC, the Cr(VI) concentration was initially decreased rapidly and gradually slowed down after four cycles of operation (Xafenias et al. 2014). An et al. (2014) studied the microbial desalination cell (MDC) to reduce Cr(VI) at cathode, and the current densities of the MDCs were also gradually decreased from the 1st cycle to the 10th cycle. While the Cr(VI) reduction efficiency of BER_{CC} reached approximately 100% after 58.5 h and 60.5 h during the 2nd and the 3rd cycle, respectively. Based on the above results, Cr(VI) could be entirely reduced for seven cycles in BER_{CC}, however, it took much longer time to reduce Cr(VI) for BER_{DC} than that for BER_{CC} (Fig. 2a). The variation of the Cr(VI) concentration in the BER_{CC} at open circuit revealed that adsorption was non-significant in the BER_{CC} (Fig. S1). Similar results were also found by Li et al. (2018). The reduction products (dark green precipitates) of Cr(VI) were found attached to the chemical cathode and sank to the bottom in BER_{CC} (Fig. S2a and Fig. S2b). Both the main constituent elements of the precipitates at the bottom of the cathodic chamber and that attached to the surface of the chemical cathode were Cr (Fig. S2 and Table S1). The main component of the precipitate in the cathodic chamber was chromium oxide (Fig. S3).

Fig. 2

3.1.2 Performance of electricity generation and sludge degradation

During seven Cr(VI) reduction cycles, the voltage of BER_{CC} was shown consistently above 0.672 V, and the maximum voltage reached about 0.813 V at the beginning of each cycle in Fig. 2b. While BER_{DC} produced high voltage only at the

beginning stage of the 1st cycle, and the voltage was gradually decreased with the Cr(VI) reduction proceeded. During the 2nd reduction cycle of BER_{DC}, the voltage was first increased slightly compared with that at the end of the 1st cycle, but it was gradually declined with the proceeding of Cr(VI) reduction. The tendency of voltage for the 5th cycle was similar to that for the previous cycles. After five cycles of a dual-chamber MFC with alumina-nickel nanoparticles-dispersed carbon nanofiber electrode, the performance of the MFC was decreased by less than 10% (Gupta et al. 2017). After 432 h of operation, the TCOD of sludge decreased by 73.6±4.4% from 27692±1662 mg/L to 7307±438 mg/L in the anodic chamber of BER_{CC} and 52.1±3.1% from 27692±1662 mg/L mg/L to 13267±796 mg/L in the anodic chamber of BER_{DC}, respectively. Of the electrons produced in organic matter degradation, a great amount were used for electricity generation, and this process could accelerate the organic matter degradation of sludge in BES (Xafenias et al. 2014). BER_{CC} can consume electrons continuously produced from the degradation of sludge. Therefore, that BER_{CC} had a higher performance of electricity generation was the main reason that the TCOD degradation of BER_{DC} was higher than that of BER_{CC} (ref. 3.1.2).

The differences between the performances of BER_{CC} and BER_{DC} in electricity generation and Cr(VI) reduction can be explained based on the electrochemical theory. According to Eq.(1), the anodic potential declined with the degradation of sludge as the Eq.(3),

$$E_{ano}=E^{0}_{ano}-\frac{RT}{nF}\ln[H^{+}]^{24} \quad (3)$$

where E_{ano} is the cathode potential, E^{0}_{ano} stands for the standard cathode potential (V), R is the ideal gas constant (8.314 J/mol K), T is the temperature (K), n is the

number of transferred electrons, F is the Faraday's constant, [H^+] is the concentrations of H^+. As Cr(VI) was reduced by the chemical cathode of BER_{DC}, the Cr(VI) concentration gradually decreased. According to Eq.(2), the electrons that transferred from the anode and participated in the chemical cathodic reaction were decreased, and the Cr(VI) reduction rate was descending slowly with it. The cathodic potential declined with the slowdown of Cr(VI) reduction rate as the Eq.(4),

$$E_{cat}=E_{cat}^{0}-\frac{RT}{nF}\ln\frac{[Cr^{3+}]^{2}}{[Cr_{2}O_{7}^{2-}][H^{+}]^{14}} \quad (4)$$

where E_{cat} is the cathode potential, E_{cat}^{0} is the standard cathode potential (V), [Cr^{3+}] and [$Cr_2O_7^{2-}$] are the concentrations of Cr(III) and Cr(VI), respectively. As indicated in Eq.(5),

$$E=E_{cat}-E_{ano} \quad (5)$$

The voltage of BER_{DC} was decreased with the operation, and the reaction of extracellular electron transfer at anode slowed down. At the beginning of the next cycle, the Cr(VI) reduction rate and cathode potential were nearly recovered at the beginning of the next cycle, however, the reaction rate of the extracellular electron transfer could not recover completely. As a consequence, the voltage of BER_{DC} gradually declined. Relevant results revealed that the decrease in performance of MES was attributed to the reduction of the catalytic activity of the electrode (Xafenias et al. 2014), which was consistent with the results of this study. On the condition of the same electrons produced at the anode and transferred to the cathode(s), though the electrons that reacted at chemical cathode decreased with the decline of Cr(VI) concentration in BER_{CC}, the electrons that reacted at the bio-cathode increased with it. Therefore, the anodic reaction could be kept at a high rate, and the voltage could be kept at a high level. A certain number of rod-shaped EAMs existed on the surface of

280 the anode, and the biofilm could be found on the bio-cathode (Fig. S1c and Fig. S1d).
281 They indicated that the EAMs maintained high activity with the cooperative cathodes
282 of chemical cathode and bio-cathode.
283
284 In summary, BER_{CC} with cooperative cathodes not only broke through the
285 limitation of Cr(VI) reduction decline during multiple cycles of operation, but also
286 produced high voltage continuously and improved sludge degradation in contrast to
287 BER_{DC}.
288
289 3.2 Impact of TCOD, Cr(VI) concentration and pH on the performance of BER_{CC}
290 The advantages of BER_{CC} on performance were preliminarily studied (ref. 3.1).
291 TCOD of excess sludge, and initial Cr(VI) concentration and pH of catholyte on the
292 performance were investigated to reflect the operation characteristics of BER_{CC} under
293 different conditions.
294
295 3.2.1 Impact of TCOD on the performance of BER_{CC}
296 Excess sludge contains abundant organic matters, so that it can provide sufficient
297 electron source for Cr(VI) reduction and electricity generation of BER_{CC}. Therefore,
298 the TCOD of the anodic substrate is not the limiting factor of the performance when
299 BER_{CC} is fueled by excess sludge. The variations of Cr(VI) reduction in BER_{CC} at
300 different TCOD (TCOD1=10769±321 mg/L, TCOD2=22307±694 mg/L, and TCOD3
301 =29692±885 mg/L) of sludge were shown in Fig. 3a, which revealed that the more the
302 TCOD in the anodic chamber, the higher the rate of Cr(VI) reduction in the chemical
303 cathodic chamber. Fig. 3b showed the polarization curves and power density curves of
304 BER_{CC} at different TCOD of sludge. After calculation, the internal resistance of

305 BER_{CC} with sludges of TCOD1, TCOD2 and TCOD3 were 151.3±5.7 Ω, 121.5±6.7 Ω,
306 140.2±7.4 Ω, respectively, since biofilms became thick gradually and the transfer
307 resistance increased at a high level of TCOD, which might have negative effects on
308 the performance of electricity generation at high TCOD level. Based on the
309 electrochemical theory, the actual cathodic potential that takes losses into
310 consideration was obtained as follows:

311 $$E_{cat}=E^{0}_{cat}-\frac{RT}{nF}\ln\frac{[Cr^{3+}]^{2}}{[Cr_{2}O_{7}^{2-}][H^{+}]^{14}}-(\eta_{oct}+\eta_{ohm}+\eta_{c}) \quad (6)$$

312 Where η_{oct}, η_{ohm}, and η_{c} stand for the activate loss(V), ohm loss(V), and mass transfer
313 loss(V), respectively. The cathodic potential is determined by the concentrations of
314 Cr(VI) and Cr(III) and pH together [Eq.(6)]. As Fig. 3b shown, both the open-circuit
315 voltage and the maximum power density were increased gradually with the increase
316 of TCOD.

317

318 Fig. 3

319

320 3.2.2 Impact of initial Cr(VI) concentration on the performance of BER_{CC}

321 On the condition of TCOD=29692±885 mg/L with the highest performance of
322 Cr(VI) reduction (ref. 3.2.1), the performances of Cr(VI) reduction in BER_{CC} at
323 different initial Cr(VI) concentrations were shown in Fig. 4a. The rate of Cr(VI)
324 reduction was increased with the increase of initial Cr(VI) concentration, since high
325 initial Cr(VI) concentration was benefit for the improvement of reduction efficiency
326 [ref. Eq.(2)]. However, the reduction rate at an initial concentration of 200 mg/L was
327 less than twice that at 100 mg/L. The possible reason was that the reaction of Cr(VI)
328 reduction was inhibited, as H^{+} was gradually consumed according to Eq.(2). As

329 calculation according to Fig. 4b, the internal resistance for 60 mg/L, 100 mg/L, 200
330 mg/L were 142.7±3.5 Ω, 122.3±4.2 Ω, and 117.1±2.9 Ω for 60 mg/L, 100 mg/L, 200
331 mg/L, respectively. Li et al. studied a dual-chamber MFC with potassium dichromate
332 as the electron acceptor. They found that the internal resistance decreased from 300 Ω
333 to 100 Ω when the Cr (VI) concentration was increased from 50 mg/L to 500 mg/L (Li
334 et al. 2009). There is no significant difference between the anodic potentials of BER_{CC}
335 at different initial Cr(VI) concentrations, which were kept about -0.20 V (vs. SHE)
336 during the reaction cycles. Cathodic potentials were increased following the growth of
337 the initial Cr(VI) concentration. Wang et al. studied that the cathodic potential
338 increased from 600 mV to 650 mV when the initial Cr (VI) concentration increased
339 from 25 mg/L to 200 mg/L, because the increased Cr(VI) concentration would
340 decrease the internal resistance of the MDC by enhancing the ionic strength and thus
341 boost the voltage of the external resistance (Wang et al. 2008). Fig. 4b showed that the
342 performances of Cr(VI) reduction rate and electricity generation were the highest
343 (7.2±0.6 W/m^3) at the initial Cr(VI) concentration of 200 mg/L.
344
345 Fig. 4
346
347 3.2.3 Impact of pH on the performance of BER_{CC}
348 At TCOD of 29692±885 mg/L and initial Cr(VI) concentration of 200 mg/L with
349 the highest performance of Cr(VI) reduction (ref. 3.2.1 and 3.2.2), the performances
350 of Cr(VI) reduction in BER_{CC} at different initial pHs were shown in Fig. 5a. During
351 the 1st Cr(VI) reduction cycle, the lower the pH value, the faster the reduction rate and
352 the higher the reduction efficiency. The reduction rates and reduction efficiencies of
353 BER at pH=1 and pH=2 were all higher than those at pH=4 [ref. Eq.(2)]. During the

354 2nd Cr(VI) reduction cycle, the reduction rate of BER_{CC} was first higher at pH=1 than
355 that of at pH=2. After a period of time, the reduction rate decreased slower at pH=1
356 than that at pH=2. In combination, the Cr(VI) reduction rate of each BER_{CC} was in the
357 order of pH 1＞pH 4＞pH 2. With the decrease of pH value, the internal resistance
358 was gradually declined as indicated in Fig. 5b. The maximum open-circuit voltage
359 were 1.054±0.045 V, 0.991±0.034 V, 0.887±0.036 V, and the maximum power density
360 were 5.2±0.4 W/m^3, 7.2±0.4 W/m^3, 9.6±0.5 W/m^3 for pH 1, pH 2, and pH 4,
361 respectively. The results indicated that the electrons were utilized much at low pH
362 with high voltage and power density obtained. An et al. (2014) studied an MDC with
363 synthetic Cr(VI) containing wastewater as the catholyte. When the pH grew up, both
364 the current density and desalination efficiency were decreased rapidly. Li et al. (2018)
365 used dual-chamber MFCs to reduce Cr(VI) and generate bioelectricity simultaneously.
366 They found that Cr(VI) reduction was fitted to the pseudo second-order model with
367 the order of rate constant pH 2> pH 3> pH 4 > pH 5 > pH 1 > pH 6 > pH 7 .
368
369 Fig. 5
370
371 3.3 Quantification of the electron fluxes
372 Analysis of electron flux could reveal the advantages of cooperative cathodes in
373 the production and utilization of electrons within BER_{CC}. In the anodic chamber,
374 electrons were produced from organic matter degradation. Electron fluxes were
375 distributed among different electron sinks (viz., current generation, exoelectrogen
376 growth, hydrogen gas production, methanogen growth, and methane production)
377 based on the electron balances and estimated (exoelectrogen and methanogen) growth
378 rates in the BER as the previous study reported (Yu et al. 2018). Most of the electrons

for current generation were transferred along the anode to the cathode and participated in the cathodic reaction with a small amount of loss.

During two Cr(VI) reduction cycles of BER_{DC}, the average TCOD degradation rate was 18.42±4.03 mg C/(L·h) [viz., mg Coulombs/(L·h)] as shown in Table 1, which contained 7.23±1.94 mg C/(L·h) for methane production, 9.59±0.43 mg C/(L·h) for biomass (exoelectrogen and methanogen) growth, and the portions for the average current production of 0.48 mA and Cr(VI) reduction rate of 1.07±0.11 mg C/(L·h). Of the electrons produced in the anodic chamber at a unit time as shown in Fig. 6, the proportion of electrons for methanogens growth, hydrogen production, methane production, and current generation (transferred along the anode) were 23.5±2.7%, 6.4±0.8%, and 33.3±3.5%, 13.3±1.7%, respectively. 77.0±6.9% of the electrons that transferred along the anode moved to chemical cathodes for Cr(VI) reduction. In contrast, the average TCOD degradation rate was 8.21±0.64 mg C/(L·h) more in BER_{CC} than that in BER_{DC}, and the electrons for the average current were increased by 0.28 mA, respectively (Table 1). These results were consistent with those in 3.1.2 and 3.1.3.

For each cycle in BER_{CC}, the Cr(VI) concentration gradually decreased with the reduction of Cr(VI) by the chemical cathode, the electrons for chemical cathode were therefore reduced, and excess electrons transferred from the anode were used for bio-cathode. Cooperative cathodes supported the high activity of EAMs (Fig. S1) instead of gradual reduction, so the Cr(VI) reduction could be continuously and efficiently maintained (Fig. 2) at the chemical cathode for the next cycle. During two operation cycles, quantification of the electron fluxes revealed that 8.21±4.03 mg

C/(L·h) more electrons were produced from organic matter degradation in BER_{CC} than those in BER_{DC}. Of them, electrons for Cr(VI) reduction was increased by 56.1±5.6%, and some electrons supported the current generation increased by 0.28 mA. The electrons for chemical cathodic reaction and bio-cathodic reaction (and loss) were increased by 51.5±4.6% and 41.1±3.7% in BER_{CC} than those in BER_{DC}, respectively (Fig. 6).

Table 1

Fig. 6

3.4 Distribution of microbial community

Microbial community analysis was to further explore why more electrons were generated by sludge in the anodic chamber and utilized for electricity generation and Cr(VI) reduction within BER_{CC} than BER_{DC}.

By the metagenomics sequencing, optimal sequences of 40993, 25543, and 35867 were obtained from the biofilms on the anode of BER_{CC}, the bio-cathode of BER_{CC}, and the anode of BER_{DC}. These samples can also be divided into 4614, 4157, and 1580 OTUs by difference, respectively. The theoretical maximum OTUs assessed by Chao1 were 12168, 9217, 12384 for the anode of BER_{CC}, bio-cathodes of BER_{CC}, and the anode of BER_{DC}, respectively. This result revealed that the bio-cathode of BER_{CC} had the highest species richness. Shannon index provides information on species richness and distribution in the community. The order of the diversity distribution was the anode of BER_{CC} (Shannon=6.633) > the bio-cathode of BER_{CC} (Shannon=6.224) > the anode of BER_{DC} (Shannon=4.172). On the other hand, the

429 results of Simpson index also revealed that the diversity of the biofilm on the anode of
430 BER_{CC} (Simpson=0.004) was higher than that on the bio-cathode of BER_{CC}
431 (Simpson=0.006) and that on the anode of BER_{DC} (Simpson=0.042).
432
433 As shown in Fig. 7, 16S rRNA microbial community structures of the biofilms
434 on the anode of BER_{CC}, the bio-cathode of BER_{CC}, and the anode of BER_{DC} were
435 analyzed and classified based on the metagenomics sequencing technology. All of the
436 three communities exhibited high diversity, where 36, 30, and 21 phyla were found in
437 the biofilms on the anode of BER_{CC}, the bio-cathode of BER_{CC}, and the anode of
438 BER_{DC}, respectively (Fig. 7a). The most significant difference was due to the different
439 proportions of Proteobacteria, Bacteroidetes, Firmicutes, Chloroflexi, Planctomycetes,
440 and Actinobacteria in their communities. A sum of the five phyla accounted for 85.0%
441 (anode of BER_{CC}), 77.5% (bio-cathode of BER_{CC}), and 98.6% (anode of BER_{DC}),
442 respectively. Chloroflexi had the lowest proportion (0.1%) in the community of
443 biofilm on the bio-cathode of BER_{CC} and the highest proportion (7.8%) in the
444 community of biofilm on the anode of BER_{CC}. Chloroflexi was enriched selectively in
445 the biofilm on the anode of BER_{CC}, which revealed that Chloroflexi might have the
446 function of transferring electrons to the anode. In the community on the anodic
447 biofilm of an MFC that operated at high temperature, Chloroflexi accounted for 12%,
448 and some bacteria belonging to Firmicutes were also verified to generate electricity
449 (Wrighton et al. 2008). Chloroflexi was also found predominant in the anodic biofilm
450 of MFC with cellulose as a substrate (Ishii et al. 2008). Though most well-known
451 EAMs (viz., *Geobacter sp.* and *Shewanella sp.*) belong to Proteobacteria,
452 Proteobacteria were richer in the biofilms on the anode of BER_{CC} (74.2%) than those
453 on the bio-cathode of BER_{CC} (49.7%) and those on the anode of BER_{DC} (48.8%).

454 Bacteroidetes are wide in distribution scope and function, and Proteobacteria and
455 Bacteroidetes have a close relationship with hydrolysis, acidity, and acetogenesis
456 (Campanaro et al. 2016). Planctomycetes and Actinobacteria were abundant in the
457 biofilms on the bio-cathode of BER_{CC}, and Planctomycetes are mainly distributed in
458 saltwater.
459
460 Fig. 7
461
462 The distribution of microbial community was shown in Fig. 7b, and 55, 61, and
463 36 classes were found in the biofilms on the anode of BER_{CC}, the bio-cathodes of
464 BER_{CC}, and the anode of BER_{DC}, respectively, which were mainly distributed to 29
465 classes. The biofilms on the anode of BER_{CC} and BER_{DC} had similar bacterial
466 community. The biofilm on the anode of BER_{CC} was concentrated in the classes of
467 β-proteobacteria (phylum of Proteobacteria), δ-proteobacteria (phylum of
468 Proteobacteria), γ-proteobacteria (phylum of Proteobacteria), α-proteobacteria
469 (phylum of Proteobacteria), Sphingobacteriia (phylum of Bacteroidetes), Clostridia
470 (phylum of Firmicutes), and Anaerolineae (phylum of Chloroflexi). The community
471 of the biofilm on the anode of BER_{DC} contained γ-proteobacteria (phylum of
472 Proteobacteria), β-proteobacteria (phylum of Proteobacteria), α-proteobacteria
473 (phylum of Proteobacteria), Sphingobacteriia (phylum of Bacteroidetes),
474 Actinobacteria (phylum of Actinobacteria) and Bacilli (phylum of Firmicutes).
475 γ-proteobacteria play important roles in the degradation of fatty acid, and the
476 digestion process (Campanaro et al. 2016). Clostridia is the functional classes during
477 the process of hydrolysis, acidity, and acetogenesis (Campanaro et al. 2016).
478 β-proteobacteria are important in the utilization of sugar alcohol (Campanaro et al.

479 2016). The proportions of δ-proteobacteria, Clostridia, and Anaerolineae in the
480 biofilms on the anodes of BER_{CC} and BER_{DC} were 9.5~17, 38~54, and 85~212 times
481 of that on the bio-cathode of BER_{CC}, respectively, which reflected the selective
482 distribution of EAMs on the anode. δ-proteobacteria was abundant in the anodic
483 biofilm of MES with high electricity generation (Lee et al. 2003; Bond et al. 2002),
484 indicating that bacteria in relation to iron reduction and electricity generation might be
485 present. Some bacteria belonging to Clostridia with the bioelectrochemical activity
486 and the character of Fe(III) reduction was isolated from MFCs (Park et al. 2003).
487
488 At the level of genus (Fig. 7c), the predominant genera in the anodic biofilm of
489 BER_{CC} were *Rhodocyclaceae* with the proportion of 16.1%, *Comamonadaceae* with
490 the proportion of 4.4%, and *Burkholderiales_incertae_sedis* with the proportion of
491 2.2% (the class of *β*-proteobacteria), *Geobacteraceae* with the proportion of 3.7% and
492 *Polyangiaceae* with the proportion of 2.7% (the class of *δ*-proteobacteria),
493 *Xanthomonadaceae* with the proportion of 3.5% (the class of *γ*-proteobacteria),
494 *Saprospiraceae* with the proportion of 5.0% and *Chitinophagaceae* with the
495 proportion of 4.1% (the class of Sphingobacteria), *Anaerolineaceae* with the
496 proportion of 4.4% (the class of Anaerolineae), *Nitrospiraceae* with the proportion of
497 3.4% (the class of Nitrospira), and *Planctomycetaceae* with the proportion of 3.2%
498 (the class of Planctomycetacia). *Rhodocyclaceae* participates in the degradation of
499 fatty acid, sulfate reduction in the process of hydrolysis and acidification, the
500 metabolism of butyrate and propionate, and denitrification, which is the main bacteria
501 of anodic biofilm without the impacts of aerobic environment (Martins et al. 2010;
502 Sun et al. 2010). *Comamonadaceae* is abundant in the anodic biofilm that can oxidize
503 the short-chain fatty acids and degrade cellulose (Rismaniyazdi et al. 2007), and it

504 could transfer electrons to the anode in MFC with organic matters and glucose as
505 substrate (Chaudhuri and Lovly 2003). *Burkholderiales_incertae_sedis* has
506 relationship with sugar alcohol utilization, degradation of fatty acid, sulfate recovery,
507 butyrate metabolism, propionate metabolism, and denitrification. *Geobacteraceae*, as
508 well-known EAMs, can transfer electrons to the anode directly. *Xanthomonas* of the
509 class γ-proteobacteria is EAMs, which was found in MFCs under different operation
510 conditions (Yu et al. 2015). *Saprospiraceae* had the function of hydrolysis in the BES
511 with excess sludge as anodic fuel (Zhang et al. 2012). *Anaerolineaceae* and *Geobacter*
512 were found the most abundant in the anodic biofilm of plant MFC (Lu et al. 2015).
513 *Anaerolineaceae* could transform saccharides of small molecules into short-chain
514 fatty acids and hydrogen (Lu et al. 2015). *Planctomycetaceae* was also found
515 abundant in MEC (Cerrillo et al. 2016). In BER_{DC}, the predominant genera included
516 *Anaerolineaceae* (the class of Anaerolineae), *Saprospiraceae* (the class of
517 Sphingobacteria), *Comamonadaceae* (the class of β-proteobacteria), *Rhodocyclaceae*
518 (the class of β-proteobacteria), *Geobacter* (the class of β-proteobacteria) and
519 *Chitinophagaceae* (the class of Sphingobacteria). The relative abundances of
520 *Comamonadaceae*, *Geobacteraceae,* and *Xanthomonadaceae* were higher in the
521 anodic biofilm of BER_{CC} than those of BER_{DC}, which implied that BER_{CC} has a
522 higher performance of electricity generation. This result was in accordance with that
523 in 3.1.2. Many EAMs were found in the anodic biofilms of BERs as shown in Table 2.
524 However, they were rarely present in the bio-cathode of BER_{CC} except for
525 *Comamonas denitrificans*. *Geobacter* was the most abundant EAM in the anodic
526 biofilm of BERs, but the typical EAM of *Shewanella* was not detected.
527
528 Table 2

529

530 The genera in the biofilm of bio-cathode in BER_{CC} were mainly
531 *Xanthomonadaceae* (the class of γ-proteobacteria), *Moraxellaceae* (the class of
532 γ-proteobacteria), *Comamonadaceae* (the class of β-proteobacteria) *Alcaligenaceae*
533 (the class of β-proteobacteria), *Bacillales_Incertae Sedis XII* (the class of
534 β-proteobacteria) , *Sphingobacteriaceae* (the class of Sphingobacteria)
535 *Chitinophagaceae* (the class of Sphingobacteria) and *Micrococcaceae* (the class of
536 Actinobacteria). *Moraxellaceae* was found enriched in BES for the treatment of
537 practical petroleum wastewater (Jain et al. 2016). *Comamonadaceae* and
538 *Alcaligenaceae* were the predominant genera in the nitrification and denitrification
539 community of MFC with dual-chamber and batch-type cathode (Sotres et al. 2016).
540 More effective cooperative cathodes than dual chemical cathodes stimulated the
541 growth of EAMs (Table 2) and produced more electrons (ref. 3.3), which enhanced
542 the performances of Cr(VI) reduction and electricity generation in BER_{CC} (ref. 3.1).
543

544 ## Conclusions

545 BER with cooperative cathodes of chemical cathode and bio-cathode (BER_{CC})
546 for improvement of Cr(VI) reduction and electricity generation were realized. The
547 specific conclusions were drawn as follows:
548 (1) The configuration of cooperative cathodes in BER_{CC} benefited from
549 preventing the decline of the performance of Cr(VI) reduction. Cr(VI) could be fully
550 reduced, and the voltage was consistently above 0.672 V for at least seven cycles in
551 BER_{CC}. The TCOD of sludge decreased by 73.6±4.4%.
552 (2) Both the Cr(VI) reduction rate and the power density were increased with the

increase of TCOD and initial Cr(VI) concentration and the decrease of pH.

(3) Quantification of the electron fluxes revealed that 8.21±4.03 mg C/(L·h) more electrons were produced from sludge degradation and 47.9±4.3% more electrons participated in cathodic reactions in BER_{CC} than those in BER_{DC}.

(4) More EAMs were found in the anodic biofilm of BER_{CC} than that of BER_{DC}, of which *Geobacter* was the most abundant.

BER_{CC} is an economical technology not only for energy production but also for treating Cr(VI) contaminated wastewater and degrading excess sludge simultaneously in electroplating industrial parks.

Author's contribution

Qingliang Zhao, Yimin Zhu: Conceptualization, Supervision, Writing- Reviewing and Editing. **Hang Yu:** Conceptualization, Methodology, Software, Writing- Original draft preparation. **Yuhui Cao:** Data curation. **Tiantian Sun:** Software. **Weifeng Liu:** Writing- Reviewing and Editing. **Zhuyuan Liang:** Methodology, Software.

Funding

The study was funded by National Nature Science Foundation of China (51908100 and 51778176), Liaoning Provincial Natural Science Foundation of China (2020-HYLH-21 and 2021-BS-070), the Fundamental Research Funds for the Central Universities (3132021160 and 3132019334), and China Postdoctoral Science Foundation (2021TQ0052).

Availability of data and materials

The datasets used and/or analyzed during the current study are available from the corresponding author on reasonable request.

Declarations

Ethics approval and consent to participate

Not applicable.

Consent for publication

Not applicable.

Competing interests

The authors declare no competing interests.

590 ## References

591 Aelterman P, Rabaey K, Pham HT, Boon N, Verstraete W (2006) Continuous
592 electricity generation at high voltages and currents using stacked microbial fuel
593 cells. Environ Sci Technol 40: 3388-3394.

594 An ZY, Zhang HC, Wen QX, Chen ZQ, Du MA (2014) Desalination combined with
595 hexavalent chromium reduction in a microbial desalination cell. Desalination 354:
596 181-188.

597 APHA (2015) Standard Methods for the Examination of Water and Wastewater, 23rd
598 ed. American Public Health Association, Standard methods for the examination
599 of water and wastewater, 23rd edn. United Book Press, Gwynn Oak.

600 Bond DR, Holmes DE, Tender LM, Lovely DR (2002) Electrode-reducing
601 microorganisms that harvest energy from marine sediments. Science 295: 483.

602 Campanaro S, Treu L, Kougias PG, Francisci DD, Valle G, Angelidaki I (2016)
603 Metagenomic analysis and functional characterization of the biogas microbiome
604 using high throughput shotgun sequencing and a novel binning strategy.
605 Biotechnol Biofuels 9: 1-17.

606 Cerrillo M, Oliveras J, Viñas MM, Bonmatí A (2016) Comparative assessment of raw
607 and digested pig slurry treatment in bioelectrochemical systems.
608 Bioelectrochemistry 110: 69-78.

609 Chaudhuri SK, Lovley DR (2003) Electricity generation by direct oxidation of
610 glucose in mediatorless microbial fuel cells. Nat Biotechnol 21: 1229-1232.

611 Chen Z, Zhu BK, Jia WF, Liang JH, Sun GX (2015) Can electrokinetic removal of
612 metals from contaminated paddy soils be powered by microbial fuel cells?
613 Environ Technol Inno 3: 63-67.

614 Gupta S, Yadav A, Verma Nishith (2017) Simultaneous Cr(VI) reduction and

615 bioelectricity generation using microbial fuel cell based on alumina-nickel
616 nanoparticles-dispersed carbon nanofiber electrode. Chem Eng J 307(1):
617 729-738.
618 Han HX, Chen S, Zhang N, Li Y, Sheng GP (2018). Visible-light-enhanced Cr(VI)
619 reduction at Pd-decorated silicon nanowire photocathode in photoelectrocatalytic
620 microbial fuel cell. Sci Total Environ 639: 1512-1519.
621 He Z, Angenent LT (2006) Application of bacterial biocathodes in microbial fuel cells.
622 Electroanal 18: 2009-2015.
623 Humphries AC, Nott KP, Hall LD, Macaskie LE (2005) Reduction of Cr(VI) by
624 immobilized cells of desulfovibrio vulgaris NCIMB 8303 and Microbacterium sp.
625 NCIMB 13776. Biotechnol Bioeng 90: 589-596.
626 Ishii S, Shimoyama T, Hotta Y, Watanabe K (2008) Characterization of a filamentous
627 biofilm community established in a cellulose-fed microbial fuel cell. BMC
628 Microbiol 8: 6.
629 Jadhav DA, Ray SG, Ghangrekar MM (2017) Third generation in bio-electrochemical
630 system research - A systematic review on mechanisms for recovery of valuable
631 by-products from wastewater. Renew Sust Energ Rev 76: 1022-1031.
632 Jain P, Srikanth S, Kumar M, Sarma PM, Singh MP, Lal B (2016) Bio-electro
633 catalytic treatment of petroleum produced water: Influence of cathode potential
634 upliftment. Bioresource Technol 219: 652-658.
635 Jiang JQ, Zhao QL, Zhang JN, Zhang GD, Lee DJ (2009) Electricity generation from
636 bio-treatment of sewage sludge with microbial fuel cell. Bioresource Technol
637 100: 5808-5812.
638 Jin W, Tolba R, Wen J, Li K, Chen A (2013) Efficient extraction of lignin from black
639 liquor via a novel membrane-assisted electrochemical approach. Electrochim

640 Acta 107: 611-618.
641 Kim CM, Lee CR, Song YE, Heo JH, Choi, SM, Lim DH, Cho J, Park C, Jang M,
642 Kim JR (2017) Hexavalent chromium as a cathodic electron acceptor in a bipolar
643 membrane microbial fuel cell with the simultaneous treatment of electroplating
644 wastewater. Chem Eng J 328: 703-707.
645 Lee J, Phung NT, Chang IS, Kim BH, Sung HC (2003) Use of acetate for enrichment
646 of electrochemically active microorganisms and their 16S rDNA analyses. FEMS
647 Microbiol Lett 223: 185-191.
648 Li M, Zhou SQ (2019) Efficacy of Cu(II) as an electron-shuttle mediator for improved
649 bioelectricity generation and Cr(VI) reduction in microbial fuel cells. Chem Eng
650 J 273: 122-129.
651 Li M, Zhou SQ, Xu YT, Liu ZJ, Ma FZ, Zhi LL, Zhou X (2018) Simultaneous Cr(VI)
652 reduction and bioelectricity generation in a dual chamber microbial fuel cell.
653 Chem Eng J 334: 1621-1629.
654 Li Y, Lu AH, Ding HR, Jin S, Yan HH, Wang CQ, Zen CP, Wang X (2009) Cr(VI)
655 reduction at rutile-catalyzed cathode in microbial fuel cells. Electrochem
656 Commun 11: 1496-1499.
657 Logan BE, Hamelers B, Rozendal R, Schröder U, Keller J, Freguia S, Aelterman P,
658 Verstraete W, Rabaey K (2006) Microbial fuel cells: Methodology and
659 technology. Environ Sci Technol 40: 5181–5192.
660 Logan BE, Regan JM (2006) Electricity-producing bacterial communities in microbial
661 fuel cells. Trends Microbiol 14: 512-518.
662 Lu L, Xing D, Ren ZJ (2015) Microbial community structure accompanied with
663 electricity production in a constructed wetland plant microbial fuel cell.
664 Bioresource Technol 195: 115-121.

665 Martins M, Faleiro ML, Chaves S, Tenreiro R, Costa MC (2010) Effect of uranium
666 (VI) on two sulphate-reducing bacteria cultures from a uranium mine site. Sci
667 Total Environ 408: 2621-2628.
668 Meng FY, Zhao QL, Zheng ZL, Wei L, Wang K, Jiang JQ, Ding J, Na XL (2019)
669 Simultaneous sludge degradation, desalination and bioelectricity generation in
670 two-phase microbial desalination cells. Chem Eng J 36: 1180-1188.
671 Pang YM, Xie DH, Wu BG, Lv ZS, Zeng XH, Wei CH, Feng CH (2013) Conductive
672 polymer-mediated Cr(VI) reduction in a dual-chamber microbial fuel cell under
673 neutral conditions. Synth Met 183(1): 57-62.
674 Park HS, Kim BH, Kim HS, Kim HJ, Kim GT, Kim M, Chang IS, Park YK, Chang HI
675 (2003) A Novel ElectrochemicallyActive and Fe(III)-reducing Bacterium
676 Phylogenetically Related to Clostridium butyricum Isolated from a Microbial
677 Fuel Cell. FEMS Microbiol Lett 223: 129-134.
678 Pratt S, Yuan ZG, Gapes D, Dorigo M, Zeng RJ, Keller J (2003) Development of a
679 novel titration and off-gas analysis (TOGA) sensor for study of biological
680 processes in wastewater treatment systems. Biotechnol Bioeng 81: 482-495.
681 Rabaey K, Angenent L, Schröder U, Keller J (2009) Bioelectrochemical Systems:
682 From Extracellular Electron Transfer to Biotechnological Application, IWA
683 Publishing: London, UK.
684 Rabaey K, Keller J (2008) Microbial fuel cell cathodes: from bottleneck to prime
685 opportunity? Water Sci Technol 57: 655-659.
686 Rabaey K, Ossieur W, Verhaege M, Verstraete W (2005) Continuous microbial fuel
687 cells convert carbohydrates to electricity. Water Sci Technol 52: 515-523.
688 Rismaniyazdi H, Christy AD, Dehority BA, Morrison M, Yu Z, Tuovinen OH (2007)
689 Electricity generation from cellulose by rumen microorganisms in microbial fuel

690 cells. Biotechnol Bioeng 97: 1398-1407.
691 Rodrigues RM, Guan X, Iñiguez JA, Estabrook DA, Chapman JO, Huang SY, Sletten
692 EM, Liu C (2019) Perfluorocarbon nanoemulsion promotes the delivery of
693 reducing equivalents for electricity-driven microbial CO_2 reduction. Nat Catal 2:
694 407-414.
695 Shi L, Dong H, Reguera G, Beyenal H, Lu A, Liu J, Yu HQ, Fredrickson JK (2016)
696 Extracellular electron transfer mechanisms between microorganisms and
697 minerals. Nat Rev Microb 14: 651-662.
698 Song TS, Jin Y, Bao J, Kang D, Xie J (2016) Graphene/biofilm composites for
699 enhancement of hexavalent chromium reduction and electricity production in a
700 biocathode microbial fuel cell. J Hazard Mater 317: 73-80.
701 Sophia AC, Saikant S (2016) Reduction of chromium(VI) with energy recovery using
702 microbial fuel cell technology. J Water Process Eng 11: 39-45.
703 Sotres A, Cerrillo M, Viñas M, Bonmatí A (2016) Nitrogen removal in a
704 two-chambered microbial fuel cell: establishment of a nitrifying-denitrifying
705 microbial community on an intermittent aerated cathode. Chem Eng J 284:
706 905-916.
707 Sun WJ, Sierra-Alvarez R, Milner L, Field JA (2010) Anaerobic oxidation of arsenite
708 linked to chlorate reduction. Appl Environ Microbiol 76: 6804-6811.
709 Virdis B, Rabaey K, Yuan Z, Rozendal RA, Keller J (2009) Electron Fluxes in a
710 Microbial Fuel Cell Performing Carbon and Nitrogen Removal. Environ Sci
711 Technol 43: 5144-5149.
712 Wan H, Yi XY, Liu XP, Feng CH, Deng Z, Wei CH (2018) Time-dependent bacterial
713 community and electrochemical characterizations of cathodic biofilms in the
714 surfactant-amended sediment-based bioelectrochemical reactor with enhanced

715 2,3,4,5-tetrachlorobiphenyl dechlorination. Environ Pollut 236: 343-354.
716 Wang G, Huang L, Zhang Y (2008) Cathodic reduction of hexavalent chromium
717 [Cr(VI)] coupled with electricity generation in microbial fuel cells. Biotechnol
718 Lett 30: 1959-1966.
719 Wang GY, Zhang BG, Li S, Yang M, Yin CC (2017) Simultaneous microbial reduction
720 of vanadium (V) and chromium (VI) by Shewanella loihica PV-4. Bioresource
721 Technol 227: 353-358.
722 Wrighton KC, Agbo P, Warnecke F, Weber KA, Brodie EL, DeSantis TZ, Hugenholtz
723 P, Andersen GL, Coates JD (2008) A novel ecological role of the Firmicutes
724 identified in thermophilic microbial fuel cells. ISME J 2: 1146-1156.
725 Xafenias N, Zhang Y, Banks CJ (2014) Evaluating hexavalent chromium reduction
726 and electricity production in microbial fuel cells with alkaline cathodes. Int J
727 Environ Sci Technol 12: 2435-2446.
728 Xie S, Liang P, Chen Y, Xia X, Huang X (2011) Simultaneous carbon and nitrogen
729 removal using an oxic/anoxic-biocathode microbial fuel cells coupled system.
730 Bioresource Technol 102(1): 348-354.
731 Yu H, Zhao QL, Dong QS, Jiang JQ, Wang K, Zhang YS (2018) Electronic and
732 metagenomic insights into the performance of bioelectrochemical reactor
733 simultaneously treating sewage sludge and Cr(VI)-laden wastewater. Chem Eng
734 J 341: 495-504.
735 Yu J, Park Y, Kim B, Lee T (2015) Power densities and microbial communities of
736 brewery wastewater-fed microbial fuel cells according to the initial substrates.
737 Bioproc Biosyst Eng 38: 85-92.
738 Zhang F, He Z (2012) Simultaneous nitrification and denitrification with electricity
739 generation in dual-cathode microbial fuel cells. J Chem Technol Biotechnol

87(1): 153-159.

Zhang GD, Zhao QL, Jiao Y, Wang K, Lee DJ, Ren NQ (2012) Efficient electricity generation from sewage sludge usingbiocathode microbial fuel cell. Water Res 46: 43-52.

Table and Figure captions

Table 1 Summary of the experimental results at the anode and cathodes during two operation cycles of BER_{CC} and BER_{DC} (ΔTCOD - the TCOD consumption rate (mg/L-C/h); ΔCH_4 - the methane production rate (mg/L-C/h); ΔH_2 - the hydrogen gas production rate (mg/L-C/h); ΔX - the biomass growth rate (mg/L-C/h); ΔX_E - the growth of exoelectrogens (mg/L-C/h); ΔX_{CH4} - the growth of methanogens).

Table 2 Relative abundance of well-known EAMs in the bacterial communities from anodes of BER_{CC} and BER_{DC}.

Fig. 1 The configurations of BER_{CC} (a) and BER_{DC} (b).

Fig. 2 Variations of Cr(VI) concentration (a), voltage (b), and TCOD (c) in BER_{CC} and BER_{DC}.

Fig. 3 The reduction of Cr(VI) (a) and the polarization curves and power density curves (b) of BER_{CC} at different TCODs of excess sludge.

Fig. 4 The reduction of Cr(VI) (a) and the polarization curves and power density curves (b) of BER_{CC} at different Cr(VI) concentrations.

Fig. 5 The reduction of Cr(VI) (a) and the polarization curves and power density curves (b) of BER_{CC} at different pHs of catholyte.

Fig. 6 Distribution of electron fluxes among different electron sinks and the electron fluxes per unit time at the anode and cathode of BER_{DC} and BER_{CC} (Anode-CH_4 - estimated electrons used for methane production at anode; Anode-H_2 - estimated electrons used for hydrogen production at anode; Anode-*I* - electrons transferred from the anode to the cathode to generate current at anode; Anode-X_{CH_4} - estimated electrons consumed for methanogen growth at anode; Anode-X_E - estimated electrons consumed for exoelectrogen

growth at anode; Bio-cathode and loss - estimated electrons transferred to bio-cathode or loss in transfer; Chemical cathode - estimated electrons transferred to chemical cathode).

Fig. 7 Relative abundances (%) of biofilm bacteria on the anode and the bio-cathode of BER_{CC} and the anode of BER_{DC} at the phyla (a), class (b) and genus level (c).

Table 1 Summary of the experimental results at the anode and cathodes during two operation cycles of BER_{CC} and BER_{DC} (ΔTCOD - the TCOD consumption rate (mg/L-C/h); ΔCH_4 - the methane production rate (mg/L-C/h); ΔH_2 - the hydrogen gas production rate (mg/L-C/h); ΔX - the biomass growth rate (mg/L-C/h); ΔX_E - the growth of exoelectrogens (mg/L-C/h); ΔX_{CH4} - the growth of methanogens).

	BER_{DC}	BER_{CC}
Cycle (h)	55.5~102.5	57.5~58.5
Current (mA)	0.48	0.66
ΔTCOD (mg C/L·h)	18.42±4.03	26.63±3.94
ΔCH_4 (mg C/L·h)	7.23±1.94	6.65±1.23
ΔCr(VI) (mg C/L·h)	1.07±0.11	1.67±0.17
ΔX (mg C/L·h)	9.59±0.43	8.59±2.23
ΔX_{CH4} (mg C/L·h)	5.18±1.23	3.18±1.23
ΔX_E (mg C/L·h)	4.41±0.67	5.31±0.72

792 **Table 2** Relative abundance of well-known EAMs in the bacterial communities from

793 anodes of BER_{CC} and BER_{DC}.

EAM	Relative abundance（%）		
	Anode of BER_{CC}	Anode of BER_{DC}	Bio-cathode of BER_{CC}
Geobacter spp.	3.7	2.2	-
Arcobacter butzlerii	0.04	0.01	1.22
Desulfovibrio denitrificans	0.01	-	-
Comamonas denitrificans	0.13	0.02	-
Desulfuromonas acetoxidans	0.02	-	-
Klebsiella pneumoniae	0.01	-	-
Rhodoferax ferrireducens	0.03	-	-

794
795
796

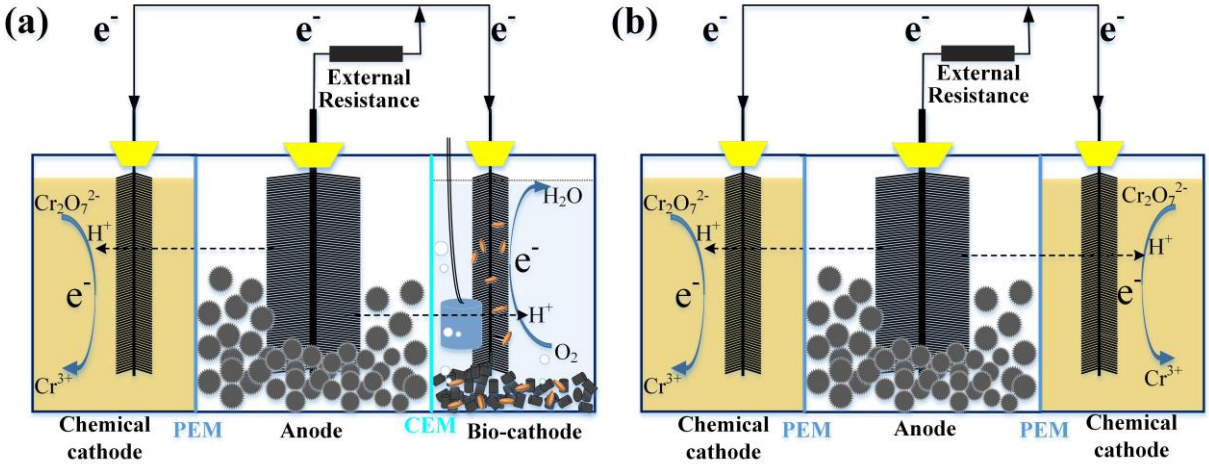

797 **Fig. 1** The configurations of BER_{CC} (a) and BER_{DC} (b).

798

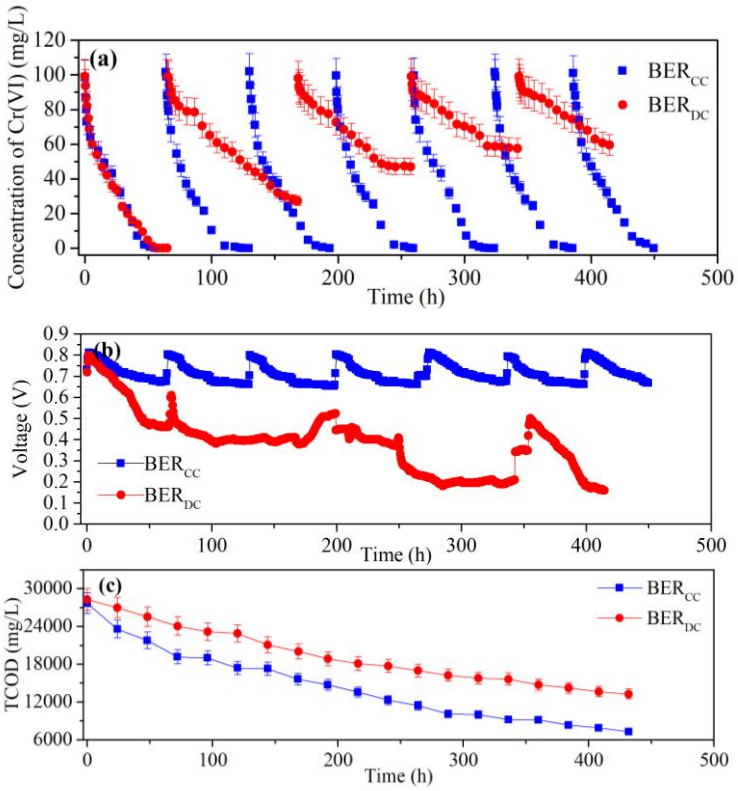

Fig. 2 Variations of Cr(VI) concentration (a), voltage (b), and TCOD (c) in BER_{CC} and BER_{DC}.

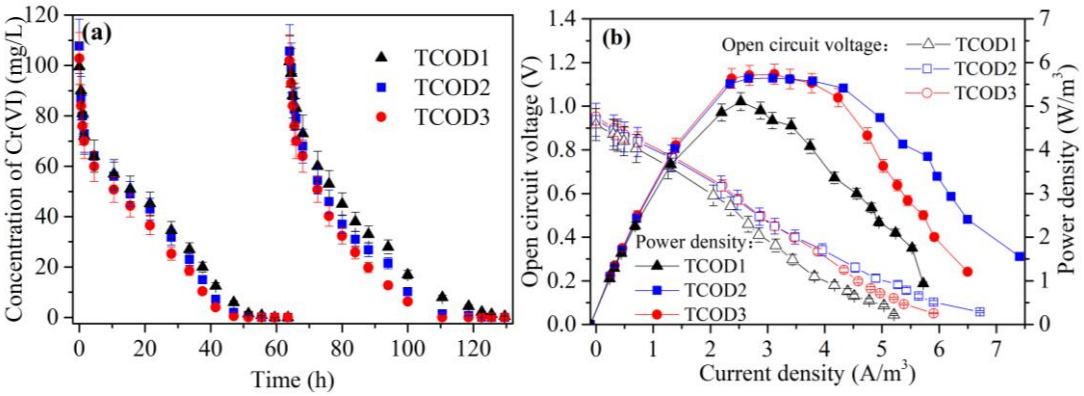

Fig. 3 The reduction of Cr(VI) (a) and the polarization curves and power density curves (b) of BER_{CC} at different TCODs of excess sludge.

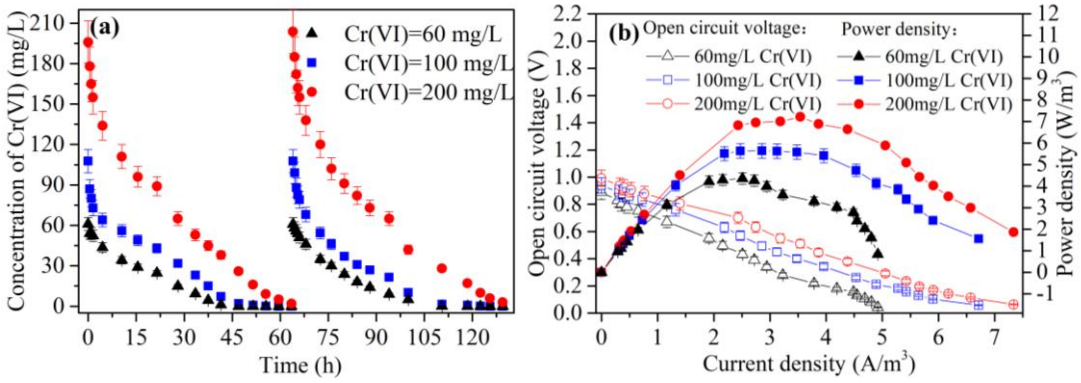

812

813

814 **Fig. 4** The reduction of Cr(VI) (a) and the polarization curves and power density

815 curves (b) of BER_{CC} at different Cr(VI) concentrations.

816

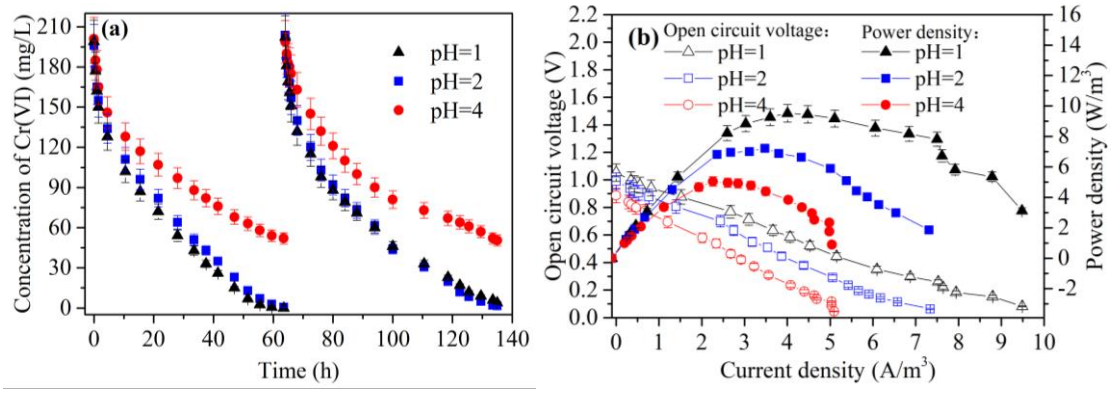

Fig. 5 The reduction of Cr(VI) (a) and the polarization curves and power density curves (b) of BER_{CC} at different pHs of catholyte.

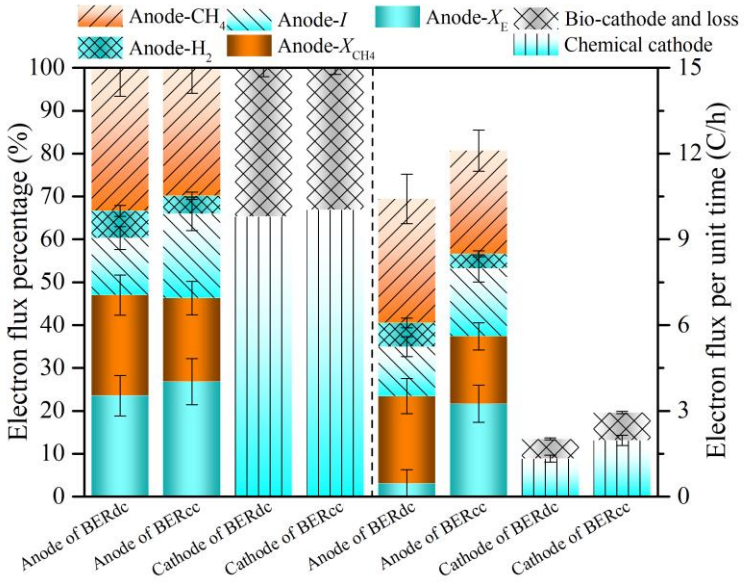

822

823 **Fig. 6** Distribution of electron fluxes among different electron sinks and the electron
824 fluxes per unit time at the anode and cathode of BER_{DC} and BER_{CC} (Anode-CH_4 -
825 estimated electrons used for methane production at anode; Anode-H_2 - estimated
826 electrons used for hydrogen production at anode; Anode-*I* - electrons transferred from
827 the anode to the cathode to generate current at anode; Anode-X_{CH4} - estimated
828 electrons consumed for methanogen growth at anode; Anode-X_E - estimated electrons
829 consumed for exoelectrogen growth at anode; Bio-cathode and loss - estimated
830 electrons transferred to bio-cathode or loss in transfer; Chemical cathode - estimated
831 electrons transferred to chemical cathode).

832

833

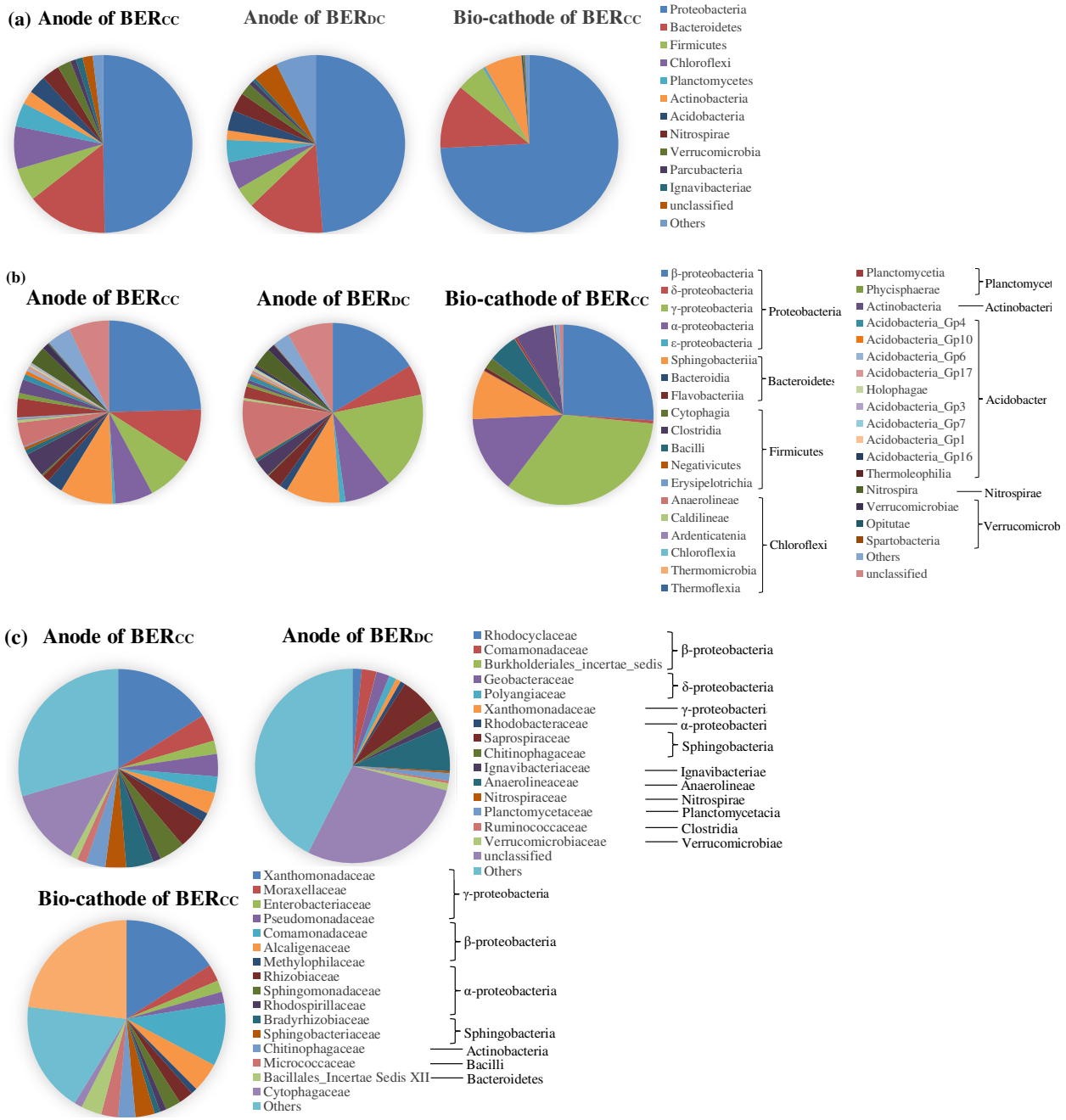

Fig. 7 Relative abundances (%) of biofilm bacteria on the anode and the bio-cathode of BER_{CC} and the anode of BER_{DC} at the phyla (a), class (b) and genus

level (c).

Supplementary Files

This is a list of supplementary files associated with this preprint. Click to download.

- Supplementarymaterial.doc